



CHALMERS
UNIVERSITY OF TECHNOLOGY

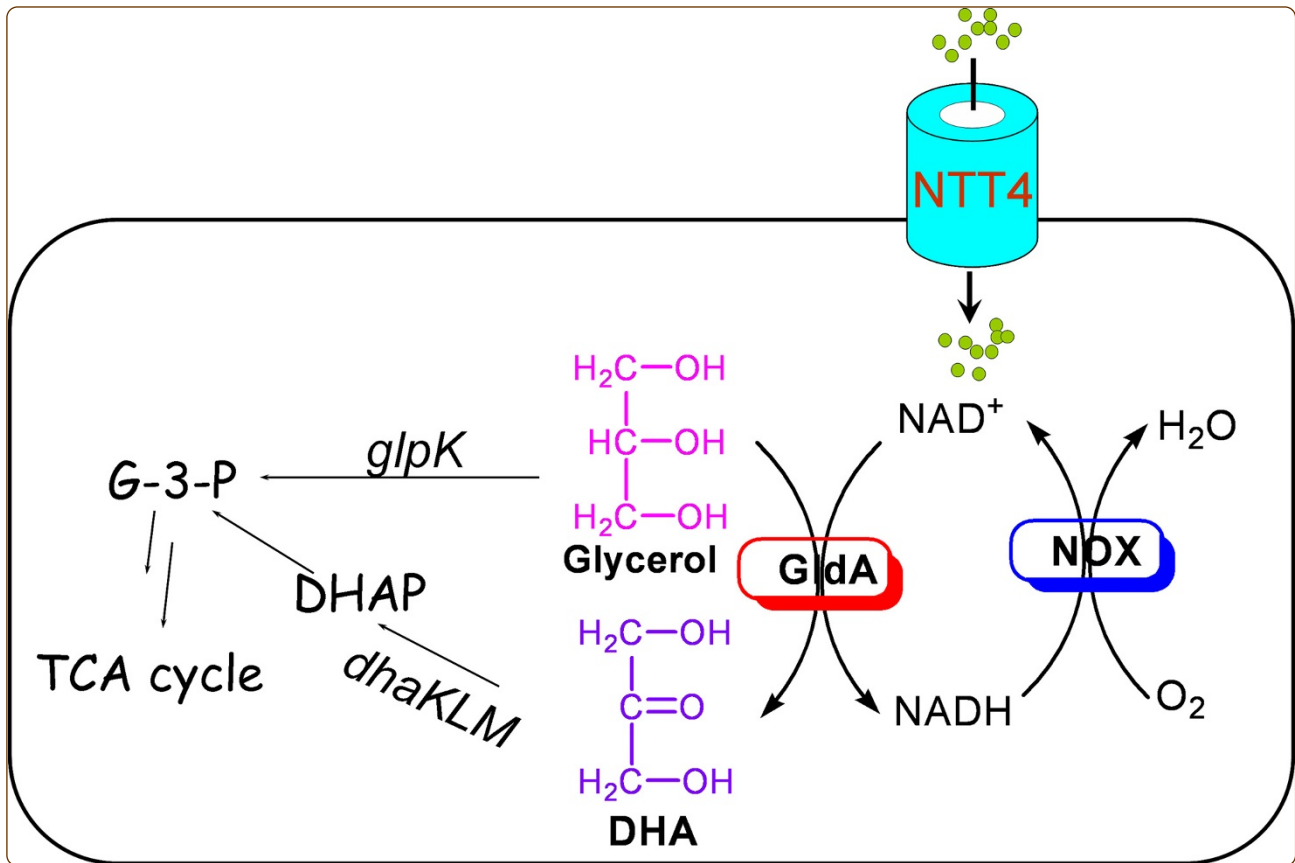
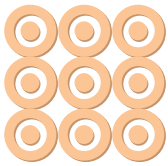
Engineering NAD⁺ availability for Escherichia coli whole-cell biocatalysis: A case study for dihydroxyacetone production

Downloaded from: <https://research.chalmers.se>, 2026-04-04 11:09 UTC

Citation for the original published paper (version of record):

Zhou, Y., Yang, W., Wang, L. et al (2013). Engineering NAD⁺ availability for Escherichia coli whole-cell biocatalysis: A case study for dihydroxyacetone production. *Microbial Cell Factories*, 12(1).
<http://dx.doi.org/10.1186/1475-2859-12-103>

N.B. When citing this work, cite the original published paper.



Engineering NAD⁺ availability for *Escherichia coli* whole-cell biocatalysis: a case study for dihydroxyacetone production

Zhou et al.

RESEARCH

Open Access

Engineering NAD⁺ availability for *Escherichia coli* whole-cell biocatalysis: a case study for dihydroxyacetone production

Yongjin J Zhou^{1,4}, Wei Yang¹, Lei Wang¹, Zhiwei Zhu¹, Sufang Zhang^{1,2} and Zongbao K Zhao^{1,2,3*}

Abstract

Background: Whole-cell redox biocatalysis has been intensively explored for the production of valuable compounds because excellent selectivity is routinely achieved. Although the cellular cofactor level, redox state and the corresponding enzymatic activity are expected to have major effects on the performance of the biocatalysts, our ability remains limited to predict the outcome upon variation of those factors as well as the relationship among them.

Results: In order to investigate the effects of cofactor availability on whole-cell redox biocatalysis, we devised recombinant *Escherichia coli* strains for the production of dihydroxyacetone (DHA) catalyzed by the NAD⁺-dependent glycerol dehydrogenase (GldA). In this model system, a water-forming NAD⁺ oxidase (NOX) and a NAD⁺ transporter (NTT4) were also co-expressed for cofactor regeneration and extracellular NAD⁺ uptake, respectively. We found that cellular cofactor level, NAD⁺/NADH ratio and NOX activity were not only strain-dependent, but also growth condition-dependent, leading to significant differences in specific DHA titer among different whole-cell biocatalysts. The host *E. coli* DH5α had the highest DHA specific titer of 0.81 g/g_{DCW} with the highest NAD⁺/NADH ratio of 6.7 and NOX activity of 3900 U. The biocatalyst had a higher activity when induced with IPTG at 37°C for 8 h compared with those at 30°C for 8 h and 18 h. When cells were transformed with the *ntt4* gene, feeding NAD⁺ during the cell culture stage increased cellular NAD(H) level by 1.44 fold and DHA specific titer by 1.58 fold to 2.13 g/g_{DCW}. Supplementing NAD⁺ during the biotransformation stage was also beneficial to cellular NAD(H) level and DHA production, and the highest DHA productivity reached 0.76 g/g_{DCW}/h. Cellular NAD(H) level, NAD⁺/NADH ratio, and NOX and GldA activity dropped over time during the biotransformation process.

Conclusions: High NAD⁺/NADH ratio driving by NOX was very important for DHA production. Once cofactor was efficiently cycled, high cellular NAD(H) level was also beneficial for whole-cell redox biocatalysis. Our results indicated that NAD⁺ transporter could be applied to manipulate redox cofactor level for biocatalysis. Moreover, we suggested that genetically designed redox transformation should be carefully profiled for further optimizing whole-cell biocatalysis.

Keywords: Cofactor engineering, NAD(H) level, NAD⁺ transporter, *Escherichia coli*, Dihydroxyacetone, Whole-cell biocatalysis

* Correspondence: zhaozb@dicp.ac.cn

¹Division of Biotechnology, Dalian Institute of Chemical Physics, CAS, Dalian 116023, China

²Dalian National Laboratory for Clean Energy, Dalian Institute of Chemical Physics, CAS, Dalian 116023, China

Full list of author information is available at the end of the article

Background

Cofactor-dependent redox biocatalysis has been shown as a powerful strategy for the production of valuable chemicals that are otherwise difficult to be synthesized [1,2]. Whole cells are preferred for industrial application because cofactors can be regenerated more efficiently [1]. To drive the redox chemistry to a specified direction, it is essential to manipulate intracellular redox state as well as cofactor levels [3]. Thus, various strategies have been applied to control the cofactor regeneration system or balance the enzyme activities of redox reactions. For example, H₂O-forming NADH oxidase (NOX) has been applied for cofactor regeneration by engineered whole-cell biocatalyst for chiral compound production [4]. The intracellular cofactor concentration was also important to attain high efficiency especially in the case that the redox enzymes had high apparent K_m values to the cofactor [5]. Previous reports showed that exogenous supplied cofactors could improve the reaction rates under whole-cell catalysis conditions, although cells were permeated and external cofactor concentrations were applied at concentrations of over 0.5 mM [6-9]. We recently found that the nucleotide transporter NTT4 encoded by the *ntt4* gene from the chlamydial endosymbiont *Protochlamydia amoebophila* UWE25 [10] could enable *Escherichia coli* cells to uptake NAD(H) from the culture broth [11]. The NAD⁺ auxotrophic *E. coli* YJE003 cells expressing NTT4 cultivated in the media containing 40 μM NAD⁺ could realize the intracellular NAD(H) pool of 5.1 mM, which was 5.8-fold more than that of the wild-type cells [11]. We reasoned that such a unique NAD(H) supplementation system could be further explored to drive cellular redox chemistry.

Glycerol has become an inexpensive and readily available commodity as a byproduct of biodiesel industry, which makes it attractive to convert glycerol into higher-value products, such as 1,3-propanediol [12], glyceric acid [13], and dihydroxyacetone (DHA) [14]. Besides the clinical and biological applications, DHA is widely used as building blocks in chemical industry and as an artificial suntan in cosmetic industry [15]. *Gluconobacter oxydans* has been shown as an excellent DHA producer by the oxidation of glycerol using the membrane-bound pyrroloquinoline quinone-dependent glycerol dehydrogenase (GDH) [16]. Native GDH contains two subunits SldA and SldB and their membrane-associated feature may cause problems for heterologous expression. In *E. coli*, the *gldA* gene (ID: 6058353) encodes an endogenous NAD⁺-dependent GDH, which catalyzes reversible reactions for the interconversion of glycerol and DHA [17]. However, GldA has higher affinity and specificity (K_m (DHA) = 0.3 mM vs. K_m (Glycerol) = 56 mM) towards DHA under normal physiological conditions, such that the conversion from DHA to glycerol ($k_{cat}/K_m = 5.7 \times$

$10^4 \text{ M}^{-1} \text{ s}^{-1}$) by GldA is far more efficient than the reverse reaction of glycerol to DHA ($k_{cat}/K_m = 4.0 \times 10^2 \text{ M}^{-1} \text{ s}^{-1}$) [17]. Here, we explored the possibility to engineer the NAD⁺ availability to reverse the GldA reaction direction for DHA production. For this purpose, we constructed recombinant *E. coli* strains that co-expressed two genes *gldA* and *nox*, and three genes *gldA*, *nox* and *ntt4*, for the production of DHA (Figure 1). Using this system as a model, we show that cellular NAD⁺ availability could be manipulated by different strategies and that the overall DHA specific titer was influenced by enzyme activity, cellular NAD⁺/NADH ratio, as well as cellular cofactor level. Our results provided useful information for the design and evaluation of redox biocatalyst to produce value-added chemicals.

Results

Construction of plasmids for DHA production

As no discernible DHA was observed when GldA alone was overexpressed in *E. coli* whole cells (date not shown), we introduced NOX as well as the NAD⁺ transporter NTT4 to increase NAD⁺ availability. Thus, two plasmids were constructed for DHA production from glycerol (Figure 1). For the plasmid pTrc99A-gldA-nox, the *gldA* gene from *E. coli* and the *nox* gene from *Enterococcus faecalis* were cloned into the vector pTrc99A with ribosome binding sites (RBS), under the control of the Trc promoter and the lacI repressor

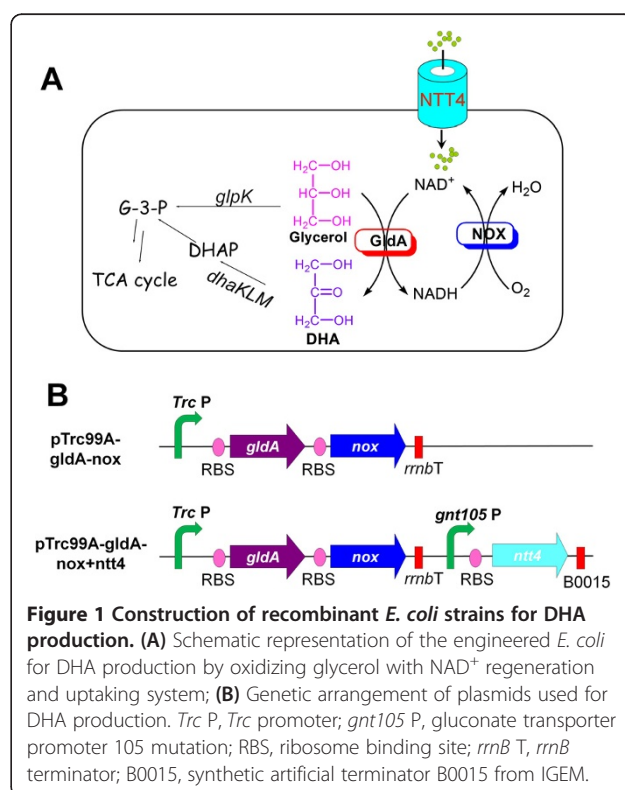


(Figure 1B). An *rrnB*T transcription terminator was located downstream of *nox*. For the plasmid pTrc99A-gldA-nox + *ntt4*, the NTT4 expression cassette in which the *ntt4* gene from *P. amoebophila* UWE25 was regulated by the promoter *gntT105* P was constructed, and inserted into the pTrc99A-gldA-nox backbone downstream of the *rrnB*T terminator using the RF cloning strategy [18]. Both plasmids ensured the expression of GldA for the oxidation of glycerol to DHA and NOX for NAD⁺ regeneration. In the case of pTrc99A-gldA-nox + *ntt4*, NTT4 was expressed to enable NAD⁺ uptake.

Strain dependence of DHA production

In *E. coli*, intracellular cofactor concentrations varied widely between different strains even under identical culture conditions in previous reports (Additional file 1: Table S1), which might affect the performance of whole-cell biocatalysts. Such phenomena may be used as a basis for host strain selection. A recent study showed that the efficiencies of different *E. coli* strains varied largely in the synthesis of (S)-1-(2-chlorophenyl)ethanol [19]. In addition, our previously constructed recombinant BL21(DE3) whole-cells produced only 0.07 g/g_{DCW} DHA without external NAD⁺ supplementation [9]. Thus, we transformed pTrc99A-gldA-nox into 6 *E. coli* strains and investigated their biocatalysis profiles (Figure 2). DHA specific titers varied greatly among different hosts (Figure 2A). Recombinant *E. coli* DH5α had the

highest DHA specific titer of 0.81 g/g_{DCW}. Recombinant DH10B and DH1 had similar specific titer of 0.08 g/g_{DCW}. However, when MG1655, BW2513 or BL21(DE3) was transformed with pTrc99A-gldA-nox, no DHA was detectable. Enzyme activity assay showed that NOX activity was well correlated with DHA titer (Figure 2B). While DH5α had a NOX activity of 3900 U/g_{DCW}, DH10B and DH1 had much lower NOX activity. NOX activities for the other three strains were below 150 U/g_{DCW}. A high NOX activity was beneficial for NAD⁺ regeneration, which was exemplified by NAD⁺/NADH ratios of different strains (Figure 2C). Indeed, DH5α, DH10B and DH1 had a relatively higher NAD⁺/NADH ratios, and the ratio reached 6.7 for DH5α. Intracellular NAD(H) levels were shown in Figure 2D. It was apparent that DH5α and DH10B had similar NAD(H) levels, and the other four strains had slightly lower yet similar values. Thus, high intracellular NAD(H) levels seemed necessary [20], but not sufficient for high DHA productivity. Instead, high initial NAD⁺/NADH ratio was well correlated with DHA titer (Figure 2A and C) and NOX activity was important to maintain high NAD⁺/NADH ratio. It remains puzzling that enzymatic activities, NAD⁺/NADH ratios and DHA productivities varied in different *E. coli* strains regardless of the presence of the same plasmid. However, similar phenomenon was reported recently that tyrosine production varied largely in 14 different *E. coli* strains containing the same pathway [21].

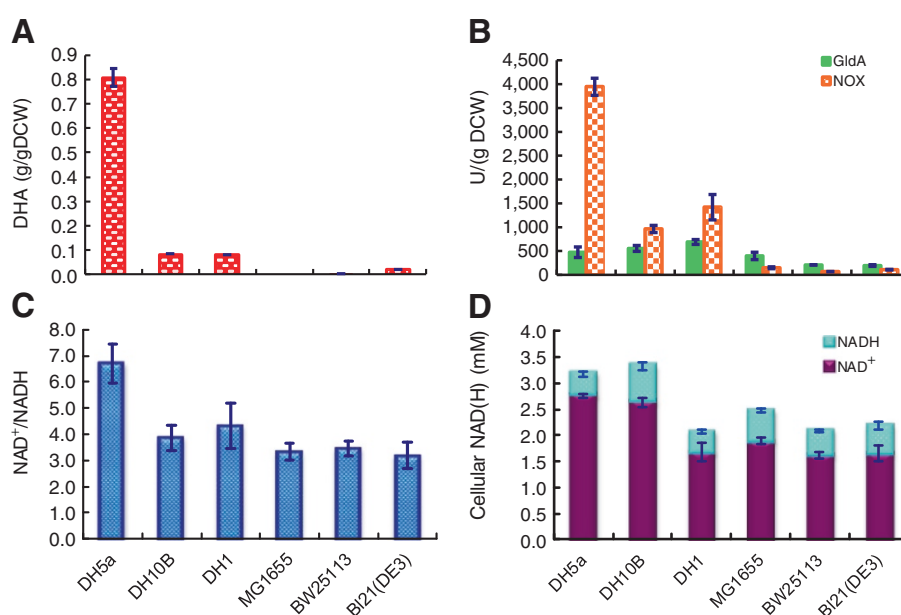


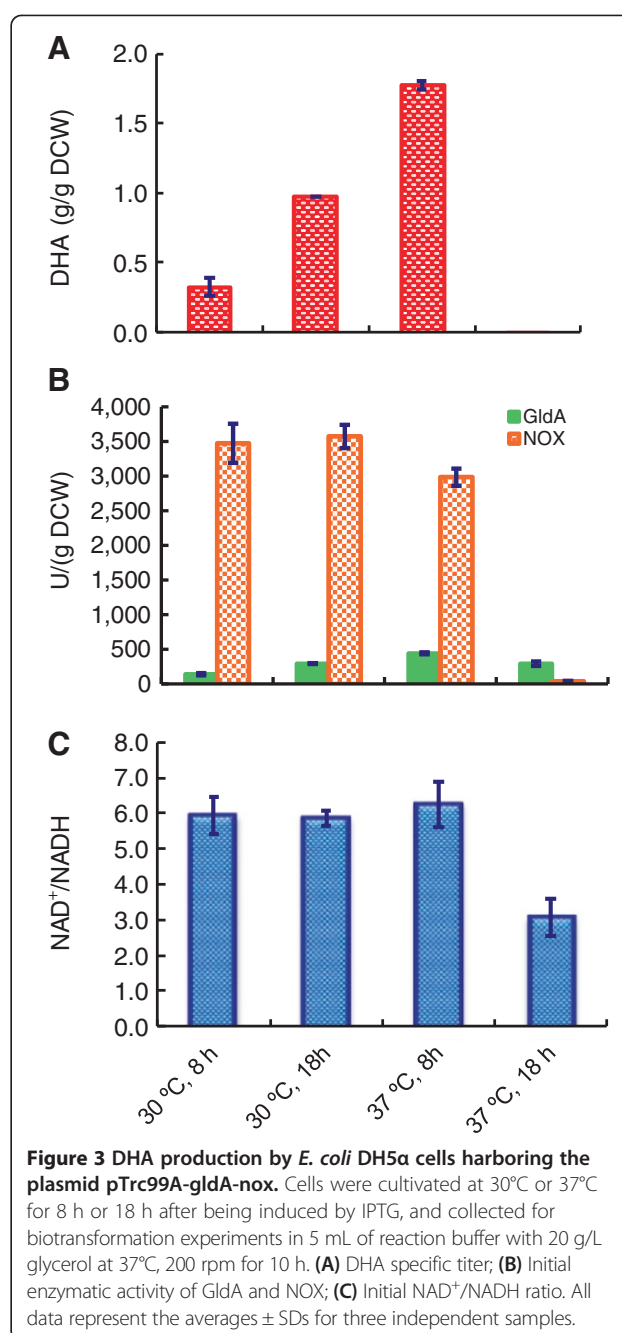
Figure 2 DHA production by different *E. coli* strains harboring the plasmid pTrc99A-gldA-nox. Cells were induced by IPTG for 20 h at 30°C, and collected for biotransformation experiments in 5 mL of reaction buffer with 20 g/L glycerol in 50-mL test tubes at 37°C, 200 rpm for 10 h. (A) DHA specific titer; (B) Initial enzymatic activity of GldA and NOX; (C) Initial NAD⁺/NADH ratio; (D) Initial intracellular NAD(H) level. The data represent the averages ± standard deviations (SDs) from three independent clones.

Effects of cell growth on DHA production

To test whether expression levels of GldA and NOX have an effect on DHA production, pTrc99A-gldA-nox transformed *E. coli* DH5 α cells were cultivated under different conditions after being induced by IPTG. At 30°C, the DHA production was increased over time to 18 h. When the cell cultivated at 37°C, the DHA production was increased when the induction time extended from 4 h (0.62 g/g DCW) to 8 h, and dropped to below detection after 12 h (Figure 3A). So we chose the representative turning time point (8 h, 18 h) for enzyme activity and NAD(H) assay and investigating their correlation with DHA production. When cells were cultivated at 30°C for 8 h or 18 h after being induced by IPTG, intracellular NOX activities were similar. However, GldA activity of 290 U/g_{DCW} for the latter sample was 2.1-fold higher than that of the former (Figure 3B). As NAD⁺/NADH ratios for both samples were also similar (Figure 3C), a higher DHA specific titer of 0.97 g/g_{DCW} for the latter was likely resulted from a higher GldA activity. When cells were cultivated at 37°C for 8 h, the highest DHA specific titer of 1.78 g/g_{DCW} was obtained together with the highest GldA activity of 440 U/g_{DCW}. The NAD⁺/NADH ratio for this sample was also slightly higher than that of the cells cultivated at 30°C. However, for the cells being cultivated at 37°C for 18 h, GldA activity, NOX activity and NAD⁺/NADH ratio were 290 U/g_{DCW}, 39 U/g_{DCW}, and 3.1, respectively, which were all substantially lower than those of other samples. As a result, DHA specific titer was only 0.01 g/g_{DCW}. The reason for a reduced NOX activity might be due to the formation of protein inclusion bodies at a higher culture temperature, because NOX overexpression was toxic to the cell [22]. These results suggested that GldA determined the catalyst efficiency in the presence of adequate NOX for NAD⁺ regeneration. Although cells were harboring an identical plasmid, these results clearly demonstrated that protein expression levels could be significantly different under varied culture conditions, leading to drastic performance differences for whole-cell biocatalysis. Similar phenomena of culture conditions affecting biocatalyst efficiency have been observed in a recent study on L-glyceraldehyde production where glucose dehydrogenase was used for NAD⁺ regeneration [7].

Promoter selection for NAD⁺ transporter expression

As has been demonstrated that intracellular NAD⁺ level and NAD⁺/NADH ratio had major effects on DHA production, we decided to further increase intracellular NAD⁺ level by NAD⁺ feeding. We [11] and others [10] showed that nucleotide transporter NTT4 could import NAD⁺ into *E. coli* cells. In this study, *ntt4* gene was cloned into vectors pBCTC and pBCTD, downstream constitutive promoters *gapA* P1 [23] and *gntT105* P



[24], to give plasmids pBCTC-*ntt4* and pBCTD-*ntt4*, respectively. Together with our previous construct pET15K-*ntt4* in which T7 promoter was used [11], three promoters were tested. These three constructs and their corresponding backbone plasmids were transformed into *E. coli* DH5 α cells. As shown in Table 1, when transformants were cultivated in the presence of 0.2 mM NAD⁺, pET15K-*ntt4* led to 7.9% intracellular NAD⁺ level increment upon IPTG induction. Similarly, pBCTC-*ntt4* led to 8.3% increment. However, pBCTD-*ntt4* transformed cells

Table 1 Intracellular NAD(H) levels of *E. coli* DH5 α cells^a harboring NTT4 expression and corresponding empty plasmids

Plasmid	Promoter	Cellular NAD(H) level (mM) ^b		Increment
		Empty vector	NTT4 expression	
pET15k	T7	1.72 \pm 0.03	1.85 \pm 0.01	7.9%
pBCTC	<i>gap</i> P1	1.96 \pm 0.00	2.13 \pm 0.01	8.3%
pBCTD	<i>gntT105</i> P	1.86 \pm 0.05	4.47 \pm 0.14	141.0%

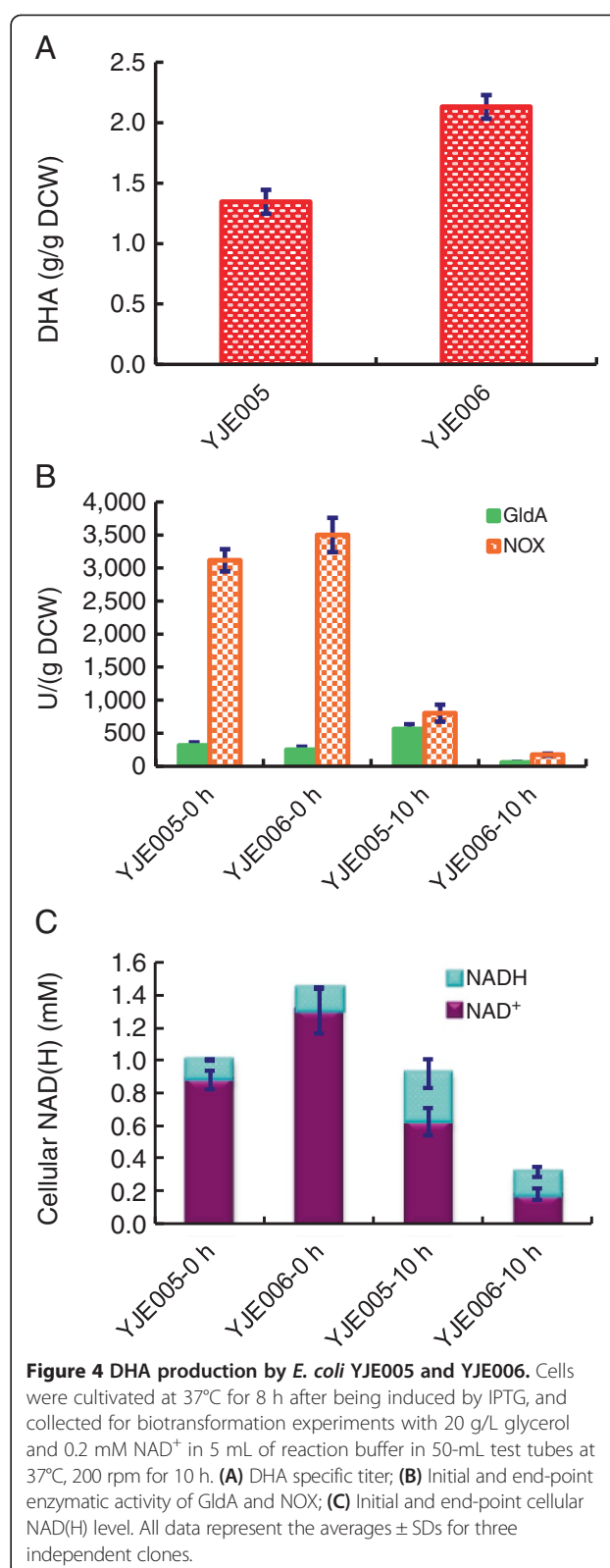
^aCells were cultivated at 37°C for 12 h in LB media containing 0.2 mM NAD⁺, collected by centrifugation and washed twice with PBS buffer.

^bAll data represent the averages \pm SDs for three independent samples.

accumulated NAD⁺ to 4.47 mM, which was 2.41-fold higher than that of pBCTD transformed cells. These results suggested that the promoter *gntT105* P was by far the most effective one in terms of NTT4 expression for NAD⁺ uptake. It should be pointed out that NTT4 is a membrane protein such that a high NTT4 expression seems toxic to the hosts which inhibited the cell growth (Additional file 1: Figure S1).

Enhancing NAD⁺ supply for DHA production by using a NAD⁺ transporter NTT4

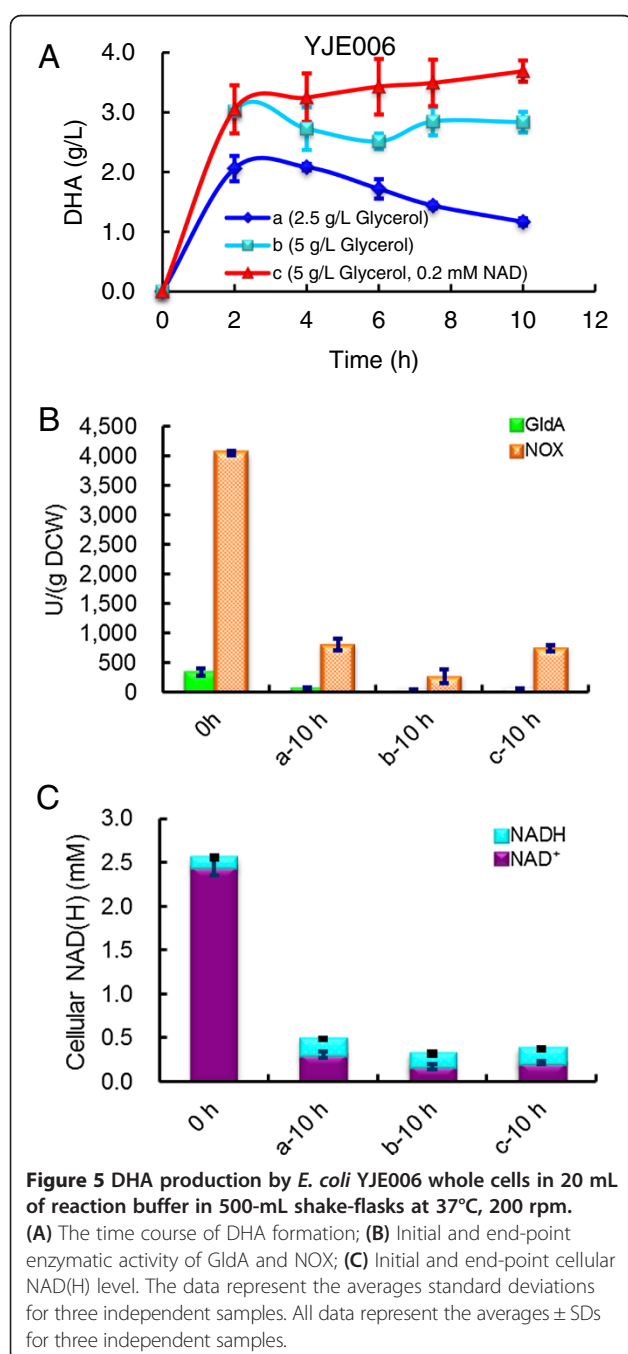
E. coli DH5 α cells were transformed with plasmids pTrc99A-gldA-nox and pTrc99A-gldA-nox + ntt4 to give strains YJE005 and YJE006, respectively. Both strains were cultivated at 37°C for 8 h in the presence of 0.2 mM NAD⁺, and whole-cell biocatalysts were prepared. DHA specific titer for YJE006 was 2.13 g/g_{DCW}, which was 1.58-fold higher than that of YJE005 (Figure 4A), suggesting that NAD⁺ feeding during the cell culture stage was beneficial to DHA production. Initial GldA activity of YJE006 (250 U/g_{DCW}) was slightly lower than that of YJE005 (310 U/g_{DCW}), while initial NOX activity of YJE006 (3500 U/g_{DCW}) was slightly higher than that of YJE005 (3100 U/g_{DCW}). After being used for 10 h, both strains had significantly reduced NOX activities. While GldA activity of YJE006 dropped to 59 U/g_{DCW}, GldA activity of YJE005, in sharp contrast, increased to 565 U/g_{DCW} (Figure 4B). Initial cellular NAD(H) level and NAD⁺/NADH ratio were 1.44 mM and 10.0 in YJE006, which were 1.44-fold and 1.34-fold higher than those of the YJE005, respectively (Figure 4C). Cellular NAD(H) level of YJE005 dropped by only 8% to 0.92 mM, but the NAD⁺/NADH ratio drastically dropped to 2.11 after 10 h. For YJE006, cellular NAD(H) level and the NAD⁺/NADH ratio were dropped by 78% and 87%, respectively, compared with those of the initial values. The fact that YJE006 cells had lower initial GldA activity but higher initial NOX activity, cellular NAD(H) level and NAD⁺/NADH ratio suggested that sufficient NAD⁺ supply and higher cellular redox state were more important than GldA activity to drive the system for DHA



production. However, YJE006 cells appeared to lose enzyme activities and cellular cofactor more rapidly than YJE005 cells.

DHA production under shake-flask conditions

In order to further investigate the NAD⁺ effect on the durability of the biocatalyst, the performance of YJE006 cells for DHA production was examined under shake-flask conditions after 2 h. When the reaction was initiated with 2.0 g_{DCW}/L cells and 2.5 g/L glycerol, DHA concentration reached 2.08 g/L after 2 h (Figure 5A, Line a) and the biocatalyst activity reached 96 U/g_{DCW}. When 5.0 g/L glycerol was used, the whole-cell catalyst produced 3.02 g/L DHA after 2 h with a higher



biocatalyst activity of 140 U/g_{DCW} (Figure 5A, Line b). In both cases, DHA concentration dropped slowly over time, suggesting that DHA may be further consumed (Figure 1A). When the reaction was initiated with 2.0 g_{DCW}/L and 5.0 g/L glycerol in the presence of 0.2 mM external NAD⁺, DHA production was burst to 3.05 g/L within 2 h, but it was slowly increasing for up to 10 h with a final titer of 3.69 g/L (Figure 5A, Line c). However, NAD⁺ supplementation failed to further improve the initial biocatalyst activity (141 U/g_{DCW}). Again, activities of GldA and NOX dropped dramatically after 10 h (Figure 5B). However, cells had higher activities of GldA and NOX as well as NAD(H) level (b-10 h vs. c-10 h) after 10 h in the presence of external NAD⁺ supplementation. These results indicated NAD⁺ feeding at the biotransformation stage was also slightly beneficial to DHA production in NTT4 expressed recombinant *E. coli* cells.

Discussion

Cellular redox state, roughly indicated by the NAD⁺/NADH ratio, is important for whole-cell redox biocatalysis. In *E. coli*, NAD⁺/NADH ratios ranging from 3 to 10 were previously documented [25]. It was expected that cellular NAD⁺/NADH ratio as well as NAD(H) level should have major effects on whole-cell biocatalysis. And co-expressing the *nox* gene encoding a H₂O-forming NOX with GldA is expected to be helpful for reversing GldA activity toward DHA biosynthesis by efficient regenerating NAD⁺. Indeed, NOX has been widely used to enhance NAD⁺-dependent biosynthesis in both resting cells [4] and growing cells [26]. In this study, we found NOX activity was not only strain-dependent (Figure 2B), but also growth condition-dependent (Figure 3B), though cells were transformed with the same plasmid pTrc99A-gldA-nox. This may be attributed to the adaption ability difference against NOX expression among these strains because high NOX activity retarded cell growth and affected the metabolism [22]. Indeed, we also found that cell growth was negatively correlated with NOX activity (date not shown). Thus, while NOX expression provided driving force to maintain a higher NAD⁺ level and cellular NAD⁺/NADH ratio, it should be carefully tuned to avoid toxic effects on cellular physiology. It was found that DHA specific titer was positively correlated with the cellular NAD⁺/NADH ratio but not the cellular NAD(H) level (Figure 2). Similarly, introducing robust cofactor regeneration system increased the whole-cell biocatalysts efficiency [19,27]. However, enhancing the cellular NADP(H) pool alone without efficient cofactor regeneration failed to improve the redox biocatalyst efficiency [28]. Together, NAD⁺/NADH ratio driven by a cofactor regeneration system is more important

than cellular cofactor level for an efficient oxidative bioreaction.

Once cofactor was efficiently regenerated, cellular cofactor level could also affect the biocatalyst efficiency [20]. External cofactor supplementation has been applied to increase intracellular NAD⁺ levels and NAD⁺/NADH ratios [6-8]. In those cases, cells were treated with permeating agents and external cofactor concentrations were high. We recently showed that NTT4 expression in *E. coli* led to uptaking NAD(H) from the culture broth [11]. Thus, *ntt4* was used to improve *E. coli* whole-cell biocatalytic efficiency by enhancing the cellular NAD(H) level. Actually, *ntt4* expression in YJE006 increased cellular NAD(H) level by 1.44 fold, indicating that NTT4 was functional in terms of uptaking external NAD⁺. As NTT4 could transport NADH efficiently [10] and increase the cellular reduction state with external NADH supplementation [11], it could also be used for increase the cellular NADH level for reduction biocatalyst such as asymmetric reduction of *o*-chloroacetophenone [8].

Although NTT4 expression strain YJE006 had a higher DHA production, it appeared to lose enzyme activities and cellular cofactor much more rapidly than YJE005. One possible reason was that NTT4 expression led to increased membrane permeability and other toxic effects. Therefore, it seemed challenging to maintain good NAD(H) durability for NTT4 expressions cells that were capable of uptaking external NAD⁺. As it requires alive cells to mediate continuous NAD⁺ transportation, NTT4 may have better potential profiting for NAD⁺-dependent multi-step biosynthesis in living cells such as 1-butanol production from glucose [29]. Although the NAD⁺ feeding strategy is cost prohibitive for bulk chemicals production, it may be useful for the production of high-value chemicals and pharmaceuticals. Alternatively, reconstruction of efficient heterologous NAD⁺ biosynthesis pathway [30] may increase cellular NAD(H) level for enhanced NAD(H)-dependent biosynthesis.

The highest specific DHA productivity reached 0.76 g/g_{DCW}/h under shake-flask conditions for the first 2 h (Figure 5A), which was lower compared with other studies of more than 2 g/g_{DCW}/h using *G. oxydans* as the hosts in small scale bioreactor [31], but much higher than that recombinant *Saccharomyces cerevisiae* of 0.03 g/g_{DCW}/h from sugar [32]. The high DHA productivity of *G. oxydans* is attributed to the membrane-bound GDH, which can directly oxidize glycerol to DHA without material transfer across cell membrane [16]. However, our attempt, in reversing an endogenous cytosolic GldA catalysis for DHA production in recombinant *E. coli* by engineering NAD⁺ availability, provided some insights on optimizing whole-cell redox biocatalyst for other valuable chemicals and pharmaceuticals production.

As DHA concentration dropped over time after 2 h, it was possible that other metabolic steps consumed DHA. In this regard, disruption of the DHA and glycerol catabolic pathway related genes such as *dhaK* and *glpK* be useful (Figure 1A). Interestingly, external NAD⁺ supplementation during the whole-cell catalysis ensured a higher NOX activity and continuous accumulation of DHA for up to 10 h. These results indicated that NOX activity was beneficial to maintain oxidative ability of the NAD⁺-dependent whole-cell biocatalysis. It is worth mentioning that the initial specific biocatalyst activity (141 U/g_{DCW}) was half to the initial GldA activity of 249 U/g_{DCW}. This might be attributed to the substrate diffusion, product consumption, etc.

In summary, using oxidation of glycerol to DHA by recombinant *E. coli* whole-cells as a model system, we enhanced oxidation state and cellular cofactor level for increasing the catalytic efficiency by expressing NADH oxidase and NAD(H) transporter, respectively. As the overall biocatalytic performance is dependent upon the cellular cofactor level, redox state and the corresponding enzymatic activity, genetically designed redox transformation should be systematically profiled to identify optimal whole-cell biocatalysis.

Material and methods

Bacterial strains and plasmids

Cloning and plasmid propagation were performed with *E. coli* DH5 α . The strains and plasmids are listed in Table 2. *E. coli* was routinely cultivated with agitation at 37°C or 30°C, 200 rpm in LB broth (10 g tryptone, 5 g yeast extract, 10 g NaCl per liter water) containing appropriate antibiotics (Kanamycin sulfate, 50 μ g/mL; ampicillin, 100 μ g/mL) if necessary.

Reagents

All primers used in this study (Table 3) were custom synthesized from Invitrogen (Shanghai, China) and DNA sequencing was performed in TaKaRa (Dalian, China). *Dpn* I, PrimeSTAR HS DNA polymerase and all other reagents for genetic manipulation were purchased from TaKaRa (Dalian, China). DNA gel purification kit and plasmid extraction kit were purchased from Beyotime (Haimen, China). All chemicals were purchased from Sigma (Shanghai, China).

DNA manipulation

The *gldA* (NCBI GeneID: 6058353) gene was amplified from *E. coli* DH5 α genomic DNA using primer pair *gldA*-F0/*gldA*-R0 and cloned into pMD18T to give pMD18T-*gldA*. The *nox* (NCBI GeneID: 1200486) gene was amplified from pMD18T-*nox*, which was constructed by cloning the *nox* gene from *Enterococcus faecalis* (CGMCC 1.130) into the pMD18T. The *gldA*-*nox*

Table 2 Strains and plasmids used in this study

Strains or plasmids	Genotype or characteristic	Resources or references
E. coli Strains		
DH5a	F ⁻ , ϕ 80d/lacZ Δ M15, Δ (lacZYA-argF)U169, <i>deoR</i> , <i>recA1</i> , <i>endA1</i> , <i>hsdR17</i> (<i>rk</i> ⁻ , <i>mk</i> ⁺), <i>phoA</i> , <i>supE44</i> , λ ⁻ , <i>thi-1</i> , <i>gyrA96</i> , <i>relA1</i>	TaKaRa
DH10B	F ⁻ , <i>mcrA</i> , Δ (<i>mrr</i> - <i>hsdRMS</i> - <i>mcrBC</i>), ϕ 80lacZ Δ M15, Δ lacX74, <i>recA1</i> , <i>endA1</i> , <i>araD139</i> , Δ (<i>ara</i> , <i>leu</i>)7697, <i>galU</i> , <i>galK</i> , λ ⁻ , <i>rpsL</i> , <i>nupG</i> /pMON14272/pMON7124	Invitrogen
DH1	F ⁻ , <i>glnV44</i> (AS), λ ⁻ , <i>rbcC1</i> , <i>gyrA96</i> (NalR), <i>recA1</i> , <i>endA1</i> , <i>thi-1</i> , <i>hsdR17</i>	CGSC (No. 6040)
MG1655	F ⁻ , λ ⁻ , <i>rph-1</i>	CGSC (No. 6300)
BW25113	<i>rrnB3</i> , Δ lacZ4787, <i>hsdR514</i> , Δ (<i>araBAD</i>)567, Δ (<i>rhaBAD</i>)568 <i>rph-1</i>	CGSC (No. 7636)
BI21(DE3)	F ⁻ , <i>dcm</i> , <i>ompT</i> , <i>hsdS</i> (rB ⁻ , mB ⁻), <i>gal</i> , λ (DE3)	Novagen
YJE005	DH5a/pTrc99A-gldA-nox	This study
YJE006	DH5a/pTrc99A-gldA-nox + ntt4	This study
Plasmids		
pMD18-T	<i>lacZ</i> , <i>pBR322 ori</i> , <i>bla</i> , cloning vector	TaKaRa
pTrc99A	<i>lacI</i> , <i>pBR322 ori</i> , <i>bla</i> , expression vector	Amersham Pharmacia
pET15K-ntt4	<i>ntt4</i> inserted within <i>NdeI</i> and <i>BamH I</i> sites, <i>kan</i>	[11]
pBCTC-ntt4	<i>ntt4</i> inserted within <i>Sac I</i> and <i>BamH I</i> sites, <i>kan</i>	This study
pBCTD-ntt4	<i>ntt4</i> inserted within <i>Sac I</i> and <i>BamH I</i> sites, <i>kan</i>	This study
pTrc99A-gldA-nox	<i>gldA</i> and <i>nox</i> transcription under <i>Trc</i> promoter	This study
pTrc99A-gldA-nox + ntt4	<i>gldA</i> and <i>nox</i> transcription under <i>Trc</i> promoter, <i>ntt4</i> under <i>gntT105p</i> promoter.	This study

Table 3 Primers used in this study^a

Primer	Sequence(5'-3')	Function
gldA-F0	TGCTGTATATAGCGCCGCAAG	<i>gldA</i> _cloning
gldA-R0	AGGTTGGTATTGGCCTGGATTTG	
gldA-F1	CAATTTACACAGGAAACAGACCATTGGACCGCATTATTCAATCAC	<i>gldA</i> _amplification
gldA-R1	GTGTATATCTCCTTCTCTAGTAGCGATCTATTATCCCACTCTTGCGAGG	
Nox-F1	CTACTAGAGAAGGAGATATACACATGAAAGTCGTAGTCGTAGG	<i>nox</i> _amplification
Nox-R1	CAAAACAGCCAAGCTTGCATGCCTGCAGTTACATATTTCTAAAGCGGCTTG	
gapAP1-F1	TCC GATATC GAGGCGAGTCAGTCGCGTAATGC	Promoter gapAP1 amplification
gapAP1-R1	ACCG GAATTC GATCTCATATGTTCCACCAGCTATTTGTTAG	
gntT105P-F1	CCGTT GATATC TGAAAGGTGTGCGCGATCTCAC	PromotergntT105P amplification
gntT105P-R1	GGAATTC TATCTCCTTATTCATTTGCGCTGGTAACGTCAATTT	
ntt4-F1	TTC GAGCTC ATGAGTAAAACAAACCAGG	
ntt4-R1	AG GGATCC TTAGTGATGATGATGATGATGTTTTTTATAAAAG	<i>ntt4</i> amplification
gntT105P-F2	CAAACCTTTTTGTTTTTTTTCTAAATACATGAAAGGTGTGCGCGATCTC	gntT105P + ntt4 amplification
ntt4-R2	CGTTTTATTTGATGCCTGGATCCGCGCTCGACTCTAGAGGATCC	
T-F1	GGATCCTCTAGAGTCGACGGATCCAGGCATCAAATAAAACG	Terminator BBa_B0015 amplification
T-R1	GTATTTAGAAAAATAAACATATAAACGCAGAAAGGCCAC	

^aThe restriction sites were bolded and the ribosome binding sites (RBS) were underlined.

co-expression cassette was constructed with the modified one-step overlap extension (SOE) PCR strategy described previously [33]. Briefly, *gldA* and *nox* were amplified with primer pairs *gldA*-F1/*gldA*-R1 and *nox*-F1/*nox*-R1, and purified *gldA* and *nox* fragments (molar ratio 1:1, about 200 ng each) were mixed. To the mixture were added 3 μ L of dNTP (2.5 mM each), 5 μ L 5 \times PrimerStar buffer, 1.25 U PrimeSTAR HS DNA polymerase, and H₂O to a total volume of 25 μ L. PCR amplification was performed according to the thermocycle conditions of 95°C for 5 min, 15 cycles of 98°C for 10 s, 68°C for 3 min, and 68°C for 10 min. Next, 2 μ L of unpurified PCR products was used as the template using the primer pair *gldA*-F1/*nox*-R1 for normal PCR amplification in a total volume of 100 μ L. The purified *gldA*-*nox* cassette was cloned into the pTrc99A using the restriction-free (RF) cloning strategy [11] to give plasmid pTrc99A-*gldA*-*nox*.

The *ntt4* (NCBI GeneID: 2780098) gene containing the 3'-end 6 \times His-tag encoding sequence was cloned from the vector pET15k-*ntt4* [11]. The constitutive glyceraldehyde-3-phosphate dehydrogenase promoter P1 *gapA* P1 [23] and the internal operator of gluconate transporter promoter 105 mutant *gntT105* P [24] was cloned from *E. coli* DH5 α genomic DNA using primer pairs *gapAP1*-F/*gapAP1*-R and *gntT105P*-F1/*gntT105P*-R1, respectively. Then, *EcoR* V-*EcoR* I digested promoters were cloned into the *EcoR* V-*EcoR* I site of pTrc99A to substitute the Trc promoter, resulting in the constitutive expression vectors pBCTA and pBCTB. The function of these two vectors was checked by constitutive expression of red fluorescent protein (date not shown). Lastly, *ntt4* was cloned into the *Sac* I-*Bam*H I site locating downstream of the constitutive promoter of pBCTA and pBCTB after cloning with the primer pair *ntt4*-F1/*ntt4*-R1, and the *bla* was replaced by the *kan* using a RF cloning strategy, resulting in plasmids pBCTC-*ntt4* and pBCTD-*ntt4*, respectively.

The *ntt4* constitutive expression cassette was also constructed and cloned into pTrc99A-*gldA*-*nox*. The *gntT105P*-*ntt4* was amplified from the pBCTD-*ntt4* using the primer pair *gntT105P*-F2/*ntt4*-R2 and terminator B0015 cloned using the primer pair T-F1/T-R1 from the international genetically engineered machine competition (IGEM, http://partsregistry.org/Part:BBa_B0015). These two DNA fragments were fused with a modified SOE PCR approach (33), and cloned into pTrc99A-*gldA*-*nox* locating downstream of the *rrnBT* terminator, resulting in plasmid pTrc99A-*gldA*-*nox* + *ntt4*.

Whole-cell biocatalyst preparation

Recombinant *E. coli* cells harboring appropriate plasmid were cultivated in LB medium supplemented with appropriate antibiotics at 37°C, 200 rpm, to the early exponential phase (OD₆₀₀ = 0.2–0.4). Cultures were induced

by adding IPTG to a final concentration of 0.1 mM (and 0.2 mM NAD⁺ if needed), and cultivated for additional 8 h or 18 h at appropriate temperature (37°C or 30°C), 200 rpm. Cells were harvested by centrifugation (2,000 g, 5 min) and washed twice with 0.1 M potassium phosphate buffer (pH 9.0).

DHA production

As *GldA* had a higher activity toward glycerol dehydrogenation [34] and our previous study [9] showed DHA production reached the highest at pH 9.0. The IPTG induced *E. coli* cells were resuspended in 5 mL of 0.1 M potassium phosphate buffer (pH 9.0) for 10 h in 5 mL of potassium phosphate buffer containing 20 g/L glycerol in 50-mL test tubes; or in 20 mL of the buffer containing 2–5 g/L glycerol in 500-mL shake flasks. NAD⁺ was added into the reaction to a final concentration of 0.2 mM when necessary. All reactions were performed at 37°C, 200 rpm. All the data represent the averages standard deviations from at least three independent samples.

DHA quantification

DHA was assayed according to a known method with minor modifications [35]. Briefly, biotransformation mixtures were centrifuged at 10,000 g for 2 min. Exactly 20 μ L of supernatants were mixed with 180 μ L diphenylamine reagent containing 1% (w/v) diphenylamine and 10% (v/v) sulfuric acid in acetic acid, and heated at 105°C for 20 min. Then, the absorbance at 620 nm were recorded after cooling to room temperature, and DHA concentrations were quantified according to a standard curve obtained under identical conditions.

Enzyme activity assay

E. coli dry cell weight (DCW) was weight by converting OD₆₀₀ value with a coefficient of 0.275 g_{DCW}/(L \times OD₆₀₀), which was determined by freezer drying the *E. coli* cells according to our recently report [36]. As the DHA production was performed at 0.1 M potassium phosphate buffer (pH 9.0) due to *GldA* activity has higher activity as mentioned above, all enzymatic assays were performed at consistent pH of 9.0. About 2 \times 10⁹ *E. coli* cells were harvested, washed twice with 0.1 M potassium phosphate buffer (pH 9.0), and stored as cell pellets at –80°C. For enzyme assays, cell pellets were resuspended in 0.2 mL of lysis buffer (10 mM Tris-Cl, 1.0 mM MgCl₂, 1 mg/mL lysozyme and 0.1 mg/mL DNase, pH 8.0) and incubated at 37°C for 30 min. *GldA* activity was estimated by recording the absorbance increase at 340 nm and assays were performed at 25°C, in 100 μ L of 0.1 M potassium carbonate buffer (pH 9.0) containing 5 mM NAD⁺, 100 mM glycerol and 5 μ L of crude cell lysates, which was with minor modifications from a previous report [37]. NOX activity

was measured by recording the absorbance decrease at 340 nm and assays were performed at 25°C, in 100 µL of 0.1 M potassium phosphate buffer (pH 9.0) containing 0.4 mM NADH and 1 µL (if the cell NOX activity was more than 1000 U/g_{DCW}) or 5 µL (if the cell NOX activity was less than 1000 U/g_{DCW}) crude cell lysates.

Cofactor measurement

Cell pellets (containing about 2×10^9 cells) were washed twice with 0.1 M potassium phosphate buffer, and then treated at 55°C for 10 min in 150 µl of 0.2 M NaOH (for NADH extraction) or 150 µl of 0.2 M HCl (for NAD⁺ extraction). The extracts were neutralized by adding 150 µl of 0.1 M HCl (for NADH extraction) or 150 µl of 0.1 M NaOH (for NAD⁺ extraction). The cellular debris was removed by centrifuging at 12,000 g for 5 min. Supernatants were transferred to new tubes and stored at -80°C until assay. NAD(H) was quantified using a sensitive enzymatic cycling assay as reported previously [11].

Additional file

Additional file 1: Table S1. Cellular NAD(H) level of different *E. coli* strains from literatures. **Figure S1.** NTT4 expression under *gntT105P* strongly retarded *E. coli* DH5a growth.

Competing interests

The authors declare that they have no competing interests.

Authors' contributions

YJZ and ZKZ conceived and designed the experiments. YJZ and WY performed the experiments. YJZ, LW, ZZ, SZ and ZKZ analyzed the data. YJZ and ZKZ wrote the manuscript. All authors read and approved the final manuscript.

Acknowledgements

We are indebted to Prof. Qin Ye (East China University of Science and Technology, China) for kindly providing pTrc99A. This work was supported by the National Basic Research and Development Program of China (No. 2012CB721103) and the State Key Laboratory of Catalysis, Dalian Institute of Chemical Physics, CAS (R201306).

Author details

¹Division of Biotechnology, Dalian Institute of Chemical Physics, CAS, Dalian 116023, China. ²Dalian National Laboratory for Clean Energy, Dalian Institute of Chemical Physics, CAS, Dalian 116023, China. ³State Key Laboratory of Catalysis, Dalian Institute of Chemical Physics, CAS, Dalian 116023, China. ⁴Present address: Department of Chemical and Biological Engineering, Chalmers University of Technology, Kemivägen 10, SE-412 96 Gothenburg, Sweden.

Received: 10 July 2013 Accepted: 5 November 2013

Published: 9 November 2013

References

- Schmid A, Dordick JS, Hauer B, Kiener A, Wubbolts M, Witholt B: **Industrial biocatalysis today and tomorrow.** *Nature* 2001, **409**:258–268.
- Jiang T, Gao C, Dou P, Ma C, Kong J, Xu P: **Rationally re-designed mutation of NAD-independent L-lactate dehydrogenase: high optical resolution of racemic mandelic acid by the engineered *Escherichia coli*.** *Microb Cell Fact* 2012, **11**:151.
- Blank LM, Ebert BE, Buehler K, Bühler B: **Redox biocatalysis and metabolism: molecular mechanisms and metabolic network analysis.** *Antioxid Redox Signal* 2010, **13**:349–394.
- Xiao Z, Lv C, Gao C, Qin J, Ma C, Liu Z, Liu P, Li L, Xu P: **A novel whole-cell biocatalyst with NAD⁺ regeneration for production of chiral chemicals.** *PLoS One* 2010, **5**:e8860.
- Bühler B, Park JB, Blank LM, Schmid A: **NADH availability limits asymmetric biocatalytic epoxidation in a growing recombinant *Escherichia coli* strain.** *Appl Environ Microbiol* 2008, **74**:1436–1446.
- Zhang J, Witholt B, Li Z: **Coupling of permeabilized microorganisms for efficient enantioselective reduction of ketone with cofactor recycling.** *Chem Commun (Camb)* 2006, **42**:398–400.
- Richter N, Neumann M, Liese A, Wohlgenuth R, Weckbecker A, Eggert T, Hummel W: **Characterization of a whole-cell catalyst co-expressing glycerol dehydrogenase and glucose dehydrogenase and its application in the synthesis of L-glyceraldehyde.** *Biotechnol Bioeng* 2010, **106**:541–552.
- Kratzer R, Pukl M, Egger S, Vogl M, Brecker L, Nidetzky B: **Enzyme identification and development of a whole-cell biotransformation for asymmetric reduction of o-chloroacetophenone.** *Biotechnol Bioeng* 2011, **108**:797–803.
- Yang W, Zhou YJ, Zhao ZK: **Production of dihydroxyacetone from glycerol by engineered *Escherichia coli* cells co-expressing *gldA* and *nox* genes.** *Afr J Biotechnol* 2013, **12**:4387–4392.
- Haferkamp I, Schmitz-Esser S, Linka N, Urbany C, Collingro A, Wagner M, Horn M, Neuhaus HE: **A candidate NAD⁺ transporter in an intracellular bacterial symbiont related to *Chlamydiae*.** *Nature* 2004, **432**:622–625.
- Zhou YJ, Wang L, Yang F, Lin XP, Zhang SF, Zhao ZK: **Determining the extremes of the cellular NAD(H) level by using an *Escherichia coli* NAD⁺-auxotrophic mutant.** *Appl Environ Microbiol* 2011, **77**:6133–6140.
- Tang X, Tan Y, Zhu H, Zhao K, Shen W: **Microbial conversion of glycerol to 1,3-propanediol by an engineered strain of *Escherichia coli*.** *Appl Environ Microbiol* 2009, **75**:1628–1634.
- Habe H, Shimada Y, Yakushi T, Hattori H, Ano Y, Fukuoka T, Kitamoto D, Itagaki M, Watanabe K, Yanagishita H, et al: **Microbial production of glyceric acid, an organic acid that can be mass produced from glycerol.** *Appl Environ Microbiol* 2009, **75**:7760–7766.
- Li MH, Wu J, Liu X, Lin JP, Wei DZ, Chen H: **Enhanced production of dihydroxyacetone from glycerol by overexpression of glycerol dehydrogenase in an alcohol dehydrogenase-deficient mutant of *Gluconobacter oxydans*.** *Bioresour Technol* 2010, **101**:8294–8299.
- Mishra R, Jain SR, Kumar A: **Microbial production of dihydroxyacetone.** *Biotechnol Adv* 2008, **26**:293–303.
- Gatgens C, Degner U, Bringer-Meyer S, Herrmann U: **Biotransformation of glycerol to dihydroxyacetone by recombinant *Gluconobacter oxydans* DSM 2343.** *Appl Microbiol Biotechnol* 2007, **76**:553–559.
- Subedi KP, Kim I, Kim J, Min B, Park C: **Role of GldA in dihydroxyacetone and methylglyoxal metabolism of *Escherichia coli* K12.** *FEMS Microbiol Lett* 2008, **279**:180–187.
- Zhou YJ, Yang F, Zhang S, Tan H, Zhao ZK: **Efficient gene disruption in *Saccharomyces cerevisiae* using marker cassettes with long homologous arms prepared by the restriction-free cloning strategy.** *World J Microbiol Biotechnol* 2011, **27**:2999–3003.
- Mädje K, Schmölzer K, Nidetzky B, Kratzer R: **Host cell and expression engineering for development of an *E. coli* ketoreductase catalyst: enhancement of formate dehydrogenase activity for regeneration of NADH.** *Microb Cell Fact* 2012, **11**:7.
- Wu X, Jiang J, Chen Y: **Correlation between intracellular cofactor concentrations and biocatalytic efficiency: coexpression of diketoreductase and glucose dehydrogenase for the preparation of chiral diol for statin drugs.** *ACS Catal* 2011, **1**:1661–1664.
- Na D, Yoo SM, Chung H, Park H, Park JH, Lee SY: **Metabolic engineering of *Escherichia coli* using synthetic small regulatory RNAs.** *Nat Biotechnol* 2013, **31**:170–174.
- Holm AK, Blank LM, Oldiges M, Schmid A, Solem C, Jensen PR, Vemuri GN: **Metabolic and transcriptional response to cofactor perturbations in *Escherichia coli*.** *J Biol Chem* 2010, **285**:17498–17506.
- Charpentier B, Branlant C: **The *Escherichia coli gapA* gene is transcribed by the vegetative RNA polymerase holoenzyme E sigma 70 and by the heat shock RNA polymerase E sigma 32.** *J Bacteriol* 1994, **176**:830–839.
- Peekhaus N, Conway T: **Positive and negative transcriptional regulation of the *Escherichia coli* gluconate regulon gene *gntB* by**

- GntR and the cyclic AMP (cAMP)-cAMP receptor protein complex. *J Bacteriol* 1998, **180**:1777–1785.
25. Leonardo MR, Dailly Y, Clark DP: Role of NAD in regulating the *adhE* gene of *Escherichia coli*. *J Bacteriol* 1996, **178**:6013–6018.
 26. Vemuri GN, Eiteman MA, Altman E: Increased recombinant protein production in *Escherichia coli* strains with overexpressed water-forming NADH oxidase and a deleted ArcA regulatory protein. *Biotechnol Bioeng* 2006, **94**:538–542.
 27. Zhang R, Xu Y, Xiao R, Zhang B, Wang L: Efficient one-step production of (S)-1-phenyl-1,2-ethanediol from (R)-enantiomer plus NAD⁺-NADPH in-situ regeneration using engineered *Escherichia coli*. *Microb Cell Fact* 2012, **11**:167.
 28. Heuser F, Schroer K, Lutz S, Bringer-Meyer S, Sahn H: Enhancement of the NAD(P)(H) pool in *Escherichia coli* for biotransformation. *Eng Life Sci* 2007, **7**:343–353.
 29. Shen CR, Lan EI, Dekishima Y, Baez A, Cho KM, Liao JC: Driving forces enable high-titer anaerobic 1-butanol synthesis in *Escherichia coli*. *Appl Environ Microbiol* 2011, **77**:2905–2915.
 30. Sorci L, Martynowski D, Rodionov DA, Eyobo Y, Zogaj X, Klose KE, Nikolaev EV, Magni G, Zhang H, Osterman AL: Nicotinamide mononucleotide synthetase is the key enzyme for an alternative route of NAD biosynthesis in *Francisella tularensis*. *Proc Natl Acad Sci USA* 2009, **106**:3083–3088.
 31. Hu ZC, Zheng YG, Shen YC: Use of glycerol for producing 1,3-dihydroxyacetone by *Gluconobacter oxydans* in an airlift bioreactor. *Bioresour Technol* 2011, **102**:7177–7182.
 32. Nguyen HT, Nevoigt E: Engineering of *Saccharomyces cerevisiae* for the production of dihydroxyacetone (DHA) from sugars: a proof of concept. *Metab Eng* 2009, **11**:335–346.
 33. Zhou YJ, Gao W, Rong Q, Jin G, Chu H, Liu W, Yang W, Zhu Z, Li G, Zhu G, *et al*: Modular pathway engineering of diterpenoid synthases and the mevalonic acid pathway for miltiradiene production. *J Am Chem Soc* 2012, **134**:3234–3241.
 34. Tang CT, Ruch FE, Lin ECC: Purification and properties of a nicotinamide adenine dinucleotide-linked dehydrogenase that serves an *Escherichia coli* mutant for glycerol catabolism. *J Bacteriol* 1979, **140**:182–187.
 35. Liu ZQ, Hu ZC, Zheng YG, Shen YC: Optimization of cultivation conditions for the production of 1,3-dihydroxyacetone by *Pichia membranifaciens* using response surface methodology. *Biochem Eng J* 2008, **38**:285–291.
 36. Wang L, Zhou YJ, Ji D, Zhao ZK: An accurate method for estimation of the intracellular aqueous volume of *Escherichia coli* cells. *J Microbiol Methods* 2013, **93**:73–76.
 37. Gonzalez R, Murarka A, Dharmadi Y, Yazdani SS: A new model for the anaerobic fermentation of glycerol in enteric bacteria: trunk and auxiliary pathways in *Escherichia coli*. *Metab Eng* 2008, **10**:234–245.

doi:10.1186/1475-2859-12-103

Cite this article as: Zhou *et al*: Engineering NAD⁺ availability for *Escherichia coli* whole-cell biocatalysis: a case study for dihydroxyacetone production. *Microbial Cell Factories* 2013 **12**:103.

Submit your next manuscript to BioMed Central and take full advantage of:

- Convenient online submission
- Thorough peer review
- No space constraints or color figure charges
- Immediate publication on acceptance
- Inclusion in PubMed, CAS, Scopus and Google Scholar
- Research which is freely available for redistribution

Submit your manuscript at
www.biomedcentral.com/submit

